

Electronic Supplementary Information (ESI)

AIE-based nanoaggregate tracker: high-fidelity visualization of lysosomal movement and drug-escaping process

Zhenxing Liu, Qi Wang,* Zhirong Zhu, Ming Liu, Xiaolei Zhao, and Wei-Hong Zhu

Shanghai Key Laboratory of Functional Materials Chemistry, Key Laboratory for Advanced Materials and Institute of Fine Chemicals, Joint International Research Laboratory of Precision Chemistry and Molecular Engineering, Feringa Nobel Prize Scientist Joint Research Center, Frontiers Science Center for Materiobiology and Dynamic Chemistry, School of Chemistry and Molecular Engineering, East China University of Science and Technology, Shanghai 200237, China.

***Corresponding authors.** E-mail: wangqi@ecust.edu.cn

Content

1. Experimental section	S3-S7
2. Images of solid TCM-PI under white light and UV light	S8
3. Absorption spectrum of TCM-PI in different solvents	S8
4. HOMO and LUMO of TCM-PI by DFT calculations	S9
5. Measurement of solution's viscosity	S9
6. Photophysical property of TCM-PI in mixtures with different viscosity	S10
7. Zeta potential of LysoTracker Red in water	S10
8. Size stability in pH 5.0 buffer solution and DMEM medium.....	S11
9. Dynamic staining process of HeLa cells.....	S11
10. Co-localization between TCM-PI nanoaggregates and LysoTracker Red	S12
11. 3D imaging of lysosomes with TCM-PI nanoaggregates	S12
12. Biocompatibility of TCM-PI nanoaggregates	S13
13. Characterization of intermediate compounds and TCM-PI	S13-S19

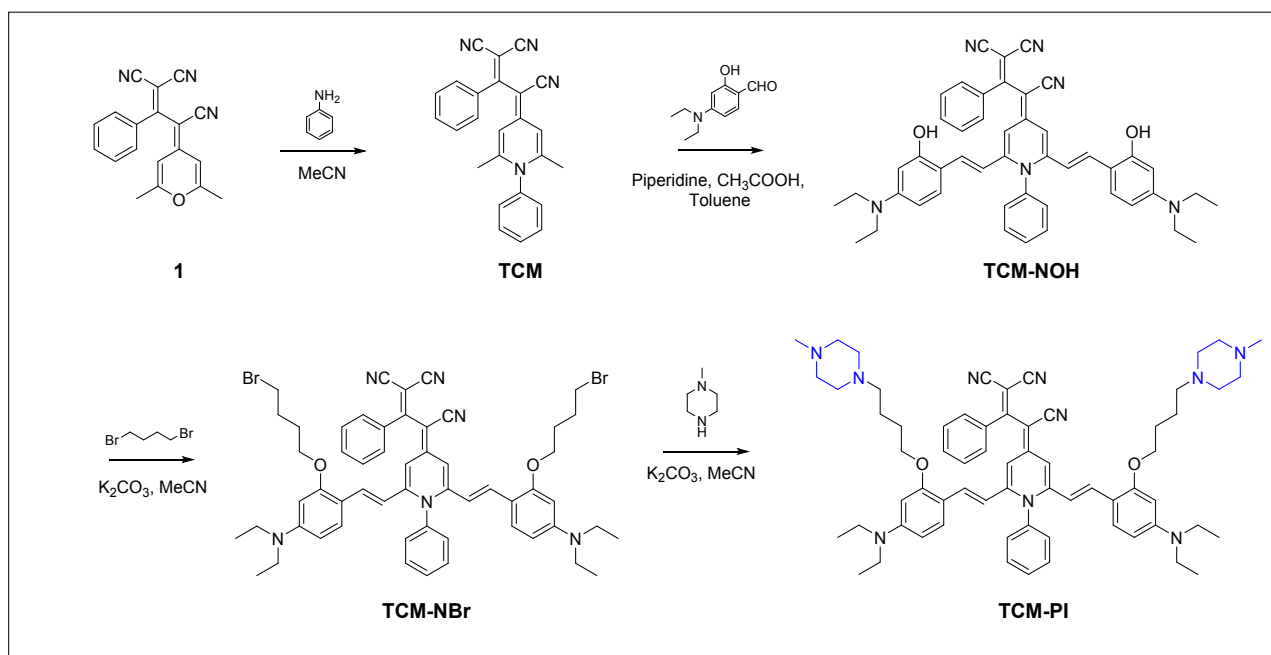
1. Experimental section

1.1 Materials and general methods

All solvents and starting reactants were purchased from commercial suppliers in analytical grade and used without purification unless special noted. The NMR spectra (^1H , ^{13}C and ^1H - ^1H COSY) were obtained from Bruker AM 400 spectrometer, using TMS ($\delta = 0$) as internal standard. Waters LCT premier XE spectrometer was used to obtain high resolution mass spectrometry (HRMS) data of the products. UV-Vis spectra and fluorescence spectra were obtained from Agilent Cary 60 spectrophotometer and F97pro fluorescence spectrophotometer respectively. Dynamic light scattering (DLS) experiments were obtained from Zetasizer Nano ZSE. The viscosity of solution was measured by TA Instruments DISCOVERY HR-2 Hybrid Rheometer. Transmission electron microscopy (TEM) images were taken on JEOL JEM-1400 instrument. Cell imaging was performed on Lecia TCS SP8 laser scanning confocal microscopy.

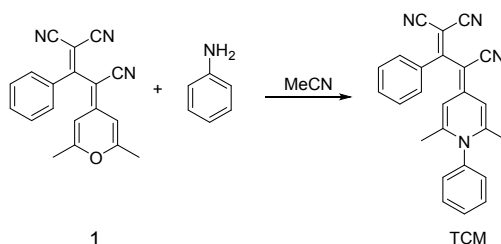
1.2 Synthesis of TCM-PI

The synthesis route of compound 1 was reported on our previous work.¹



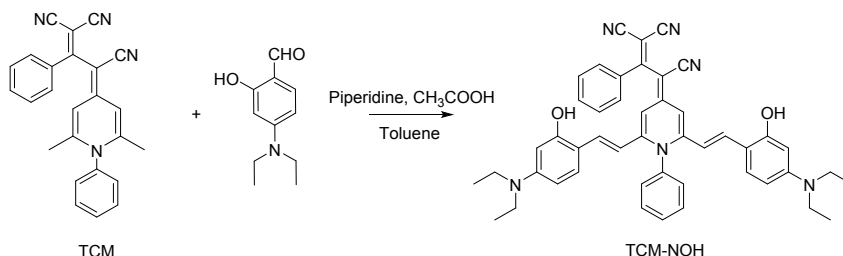
Scheme S1. Synthetic route of compound TCM-PI.

Synthesis of TCM



Compound 1 (3.00 g, 10.02 mmol), acetonitrile (30 mL) and aniline (5.60 g, 60.13 mmol) were added into a two-neck flask. The mixture was refluxed under nitrogen atmosphere for 10 h. After the mixture was cooled to room temperature, solvent was removed under reduced pressure. Crude product was further purified by silica gel chromatography with dichloromethane/methanol (v/v, 300:1) to afford orange solid (2.65 g, 71% yield). ^1H NMR (400 MHz, $\text{DMSO}-d_6$, ppm): δ 7.71-7.46 (m, 10H, Ph-H), 7.02 (s, 2H, alkene-H), 2.05 (s, 6H, $-\text{CH}_3$). ^{13}C NMR (100 MHz, $\text{DMSO}-d_6$, ppm): δ 166.16, 152.91, 150.80, 138.23, 136.53, 131.30, 130.49, 130.43, 130.12, 128.96, 126.69, 119.69, 118.72, 118.11, 116.65, 79.61, 60.81, 21.35. Mass spectrometry (ESI positive ion mode for $[\text{M}+\text{H}]^+$): Calc. for $\text{C}_{25}\text{H}_{19}\text{N}_4$: 375.1610; found: 375.1608.

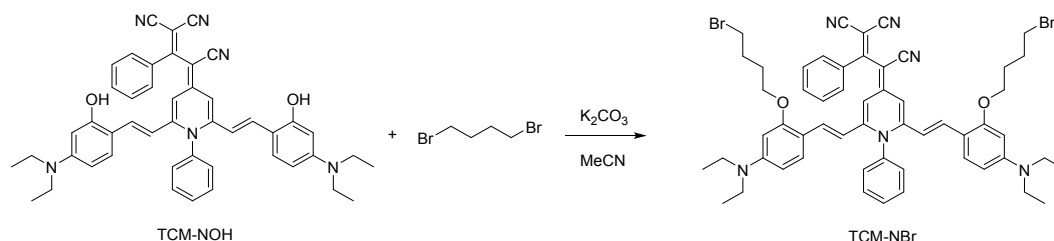
Synthesis of TCM-NOH



Piperidine (0.50 mL) and acetic acid (0.25 mL) was added dropwise to the mixture of TCM (0.80 mg, 2.14 mmol), 4-(diethylamino) salicylaldehyde (4.14 g, 21.40 mmol) and toluene (25 mL). The mixture was refluxed under nitrogen atmosphere for 12 h. After the mixture was cooled to room temperature, solvent was removed under reduced pressure. The solid was dissolved in 100 mL dichloromethane, and the solution was washed with brine (100 mL*3) for three times. The organic phase is dried with anhydrous sodium sulfate, and dichloromethane was removed under reduced pressure. Crude product was further purified by silica gel chromatography with dichloromethane/methanol (v/v, 50:1) to afford black solid (0.96 g, 62% yield). ^1H NMR (400 MHz, $\text{DMSO}-d_6$, ppm): δ 9.80 (broad, 2H, $-\text{OH}$), 7.74-7.63 (m, 3H, Ar-H), 7.61-7.53 (m, 5H, Ar-H), 7.44-7.37 (m, 2H, Ar-H), 7.17-6.66 (m, 6H, Ar-H), 6.27-6.09 (m, 4H, $J = 15.76$ Hz for alkene-H), 6.06 (s, 2H, alkene-H), 3.28 (q, 8H, $J = 6.84$ Hz, $\text{N}-\text{CH}_2-\text{CH}_3$), 1.05 (t, 12H, $J = 6.88$ Hz, $\text{N}-\text{CH}_2-\text{CH}_3$). ^{13}C NMR (100 MHz, $\text{DMSO}-d_6$, ppm): δ 165.17,

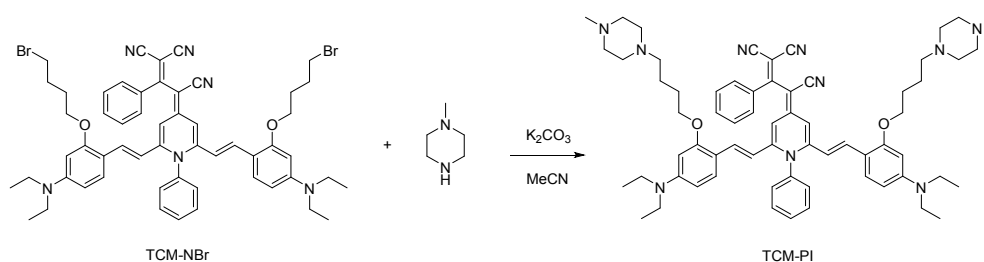
158.55, 150.57, 150.48, 150.14, 138.10, 136.60, 135.30, 131.09, 130.87, 130.45, 130.26, 130.11, 129.19, 127.77, 119.02, 117.10, 112.75, 112.48, 109.98, 104.10, 97.33, 80.20, 43.85, 12.51. Mass spectrometry (ESI positive ion mode for $[M+H]^+$): Calc. for $C_{47}H_{45}N_6O_2$: 725.3604; found: 725.3615.

Synthesis of TCM-NBr



TCM-NOH (350 mg, 0.48 mmol), 1,4-dibromobutane (1043 mg, 4.83 mmol) and anhydrous potassium carbonate (665 mg, 4.81 mmol) were stirred in acetonitrile (15 mL) at 80 °C under nitrogen atmosphere for 12 h. After it was cooled to room temperature, potassium carbonate was removed through filtration. The solvent was removed under reduced pressure, and black crude product was obtained. The product was further purified by silica gel chromatography with dichloromethane/methanol (v/v, 100:1) to afford black solid (199 mg, 42% yield). 1H NMR (400 MHz, $CD_2Cl_2-d_2$, ppm): δ 7.71-7.61 (m, 5H, Ar-H), 7.60-7.50 (m, 3H, Ar-H), 7.41-7.14 (m, 6H, Ar-H), 6.96 (d, 2H, J = 8.72 Hz, alkene-H), 6.32-6.09 (m, 4H, alkene-H and Ar-H, J = 15.36 Hz for alkene-H), 6.01 (s, 2H, alkene-H), 3.92 (t, 4H, J = 6.24 Hz, $O-CH_2-$), 3.51 (t, 4H, J = 6.48 Hz, $-CH_2-Br$), 3.36 (q, 8H, J = 7.00 Hz, $N-CH_2-CH_3$), 2.01-1.92 (m, 4H, $-CH_2-CH_2-Br$), 1.85-1.73 (m, 4H, $-O-CH_2-CH_2-$), 1.15 (t, 12H, J = 7.04 Hz, $N-CH_2-CH_3$). ^{13}C NMR (100 MHz, $CD_2Cl_2-d_2$, ppm): δ 166.37, 159.81, 151.84, 151.28, 151.01, 139.11, 138.10, 135.65, 131.53, 131.33, 131.00, 130.96, 130.64, 129.30, 128.45, 120.90, 119.38, 117.95, 114.54, 114.20, 112.04, 104.80, 94.86, 81.90, 67.46, 45.02, 34.35, 29.78, 27.97, 12.81. Mass spectrometry (ESI positive ion mode for $[M+H]^+$): Calcd. for $C_{55}H_{59}Br_2N_6O_2$: 993.3066; found: 993.3060.

Synthesis of TCM-PI



1-methylpiperazine (300 mg, 3.00 mmol) was added dropwise to the mixture of TCM-NBr (150 mg, 0.15 mmol), anhydrous potassium carbonate (207 mg, 1.50 mmol) and acetonitrile (15 mL). The

mixture was refluxed under nitrogen atmosphere for 12 h. After it was cooled to room temperature, potassium carbonate was removed through filtration. The solvent was removed under reduced pressure. Black solid was dissolved in 75 mL dichloromethane, and the solution was washed with brine (75 mL*3) for three times. The organic phase was dried with anhydrous sodium sulfate, and dichloromethane was removed under reduced pressure. The crude product was further purified by silica gel chromatography with dichloromethane/methanol (v/v, 20:1) to afford black solid (90 mg, 58%). ¹H NMR (400 MHz, CD₂Cl₂-d₂, ppm): δ 7.67-7.60 (m, 5H, Ar-H), 7.60-7.51 (m, 3H, Ar-H), 7.35-7.11 (m, 6H, Ar-H), 6.94 (d, 2H, *J*=8.84 Hz, alkene-H), 6.17 (d, 2H, *J*=15.60 Hz, alkene-H), 6.17 (d, 2H, *J*=2.12 Hz, Ar-H), 6.01 (d, 2H, *J*=2.08 Hz, Ar-H), 3.89 (t, 4H, *J*=6.34 Hz, O-CH₂-), 3.36 (q, 8H, *J*=7.08 Hz, N-CH₂-CH₃), 2.66-2.41 (m, 20H, N-CH₂-CH₂-), 2.30 (s, 6H, N-CH₃), 1.70-1.55 (m, 8H, -CH₂-CH₂-CH₂-), 1.15 (t, 12H, *J*=7.08 Hz, N-CH₂-CH₃). ¹³C NMR (100 MHz, CD₂Cl₂-d₂, ppm): δ 166.38, 160.02, 151.84, 151.35, 151.03, 139.10, 138.00, 135.84, 131.70, 131.32, 130.98, 130.97, 130.60, 129.38, 128.41, 120.84, 119.42, 117.94, 114.39, 114.18, 112.05, 104.67, 94.91, 81.69, 68.27, 58.09, 54.96, 52.87, 45.74, 45.71, 45.01, 27.37, 23.35, 12.84. Mass spectrometry (ESI positive ion mode for [M+H]⁺): Calcd. for C₆₅H₈₁N₁₀O₂: 1033.6544; found: 1033.6537.

1.3 Cell culture

Human epithelioid cervical carcinoma (HeLa) cells were purchased from the Institute of Cell Biology (Shanghai, China). Cells were propagated in cell culture flask at 37 °C under humidified 5% CO₂ atmosphere. Dulbecco's modified eagle medium (DMEM, GIBCO/Invitrogen, Camarillo, CA, USA) was supplemented with 1 % (Vol %) penicillin-streptomycin (10,000 U mL⁻¹ penicillin, and 10 mg mL⁻¹ streptomycin, Solarbio life science, Beijing, China) and 10% (Vol %) fetal bovine serum (FBS, Biological Industry, Kibbutz Beit Haemek, Israel).

1.4 Co-localization experiment

HeLa cells at the density of 2×10⁵ cells/well were seeded onto glass bottom cell culture dish (Φ 20 mm, NEST) and then cultured for 12 h. Then, the culture medium was removed, and HeLa cells were incubated with TCM-PI (3 μM) at 37 °C for 30 min. Next, the culture medium containing TCM-PI was removed, and these cells were washed with PBS for three times. Following that, these HeLa cells were incubated with commercial tracker (LysoTracker Green 100 nM, LysoTracker Red 100 nM, MitoTracker Green 100 nM and ER-Tracker Green 1 μM) at 37 °C for 30 min. After washed with PBS for three times, HeLa cells were imaged by confocal laser scanning microscope (Leica TCS SP8, 63 × oil lens).

1.5 Cytotoxicity assay

MTT assays were used to assess the cell viability of TCM-PI. HeLa cells were seeded in a 96-well

culture at the density of 5×10^3 per well, and these cells were cultured at 37 °C with humidified 5% CO₂ for 12 h. The culture medium was replaced with 100 µL fresh medium containing different concentration of TCM-PI (20 µM, 10 µM, 5 µM, 2.5 µM, 1 µM, 0 µM), and further incubating these cells for 24 h. After that, MTT solution (10 µL, 5 mg mL⁻¹) was added into each well, followed by incubation for another 4 h. 100 µL of solubilization solution containing 10% SDS and 0.01 mol/L HCl was added to dissolve the purple crystals. After 12 h incubation, the absorbance of MTT at 490 nm was monitored by the microplate reader (Bio-Rad iMark), and the TCM-PI with same incubation concentration to each sample was detected as the background. These cells without any treatment were used as control. The relative cell viability was calculated by the equation: cell viability (%) = $(OD_{\text{treated}} - OD_{\text{background}} / OD_{\text{control}}) \times 100\%$.

1.6 Photostability of TCM-PI

TCM-PI, LysoTracker Red and Indocyanine green (ICG) were diluted in DMSO at concentration of 1 µM. The absorption spectrum of each part was recorded at the beginning, following by exposing to light (11 mW cm⁻², Hg/Xe lamp) on a magnetic stirrer. The absorption spectrum was recorded at regular time intervals, and the photostability experiment was repeated three times independently.

1.7 Transmission electron microscopy imaging

10 µL TCM-PI (dilluted in pure water to concentration of 10 µM) was added onto a carbon-coated copper grid (Electron Microscopy Services, Hatfield, PA), followed by drying at room temperature overnight. The TEM imaging was performed on JEOL JEM-1400 with an accelerating bias voltage of 100 kV.

1.8 Quantum yield of TCM-PI

Table S1. Absolute quantum yield of TCM-PI in nanoaggregates and solid state

	Nanoaggregates ^[b]	Solid
Absolute Quantum Yield ^[a]	0.7 %	1.6 %

[a] Absolute quantum yield was measured by HAMAMATSU Quantaurus-QY C11347-11. λ_{ex} =514 nm. [b] Absolute quantum yield in nanoaggregates was measured in 99% (Vol %) water, and concentration of TCM-PI is 10 µM.

2. Images of solid TCM-PI under white light and UV light

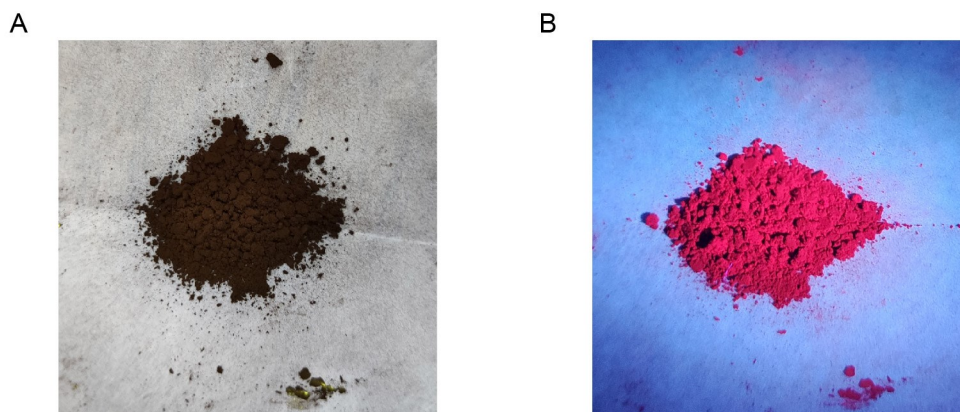


Fig. S1 Images of solid TCM-PI under (A) LED white light and (B) UV lamp at 365 nm.

3. Absorption spectrum of TCM-PI in different solvents

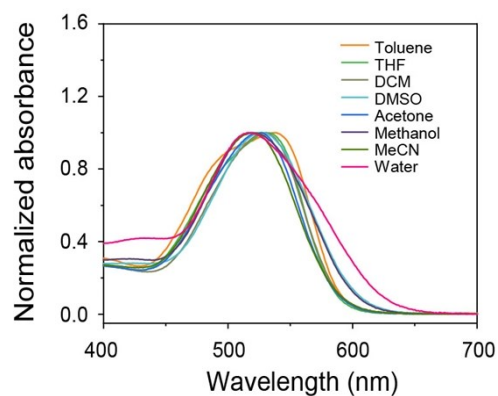


Fig. S2 Absorption spectrum of TCM-PI (10 μ M) in different solvent. TCM-PI exhibited similar absorption bands with absorption peak located at around 525 nm.

4. HOMO and LUMO of TCM-PI by DFT calculations

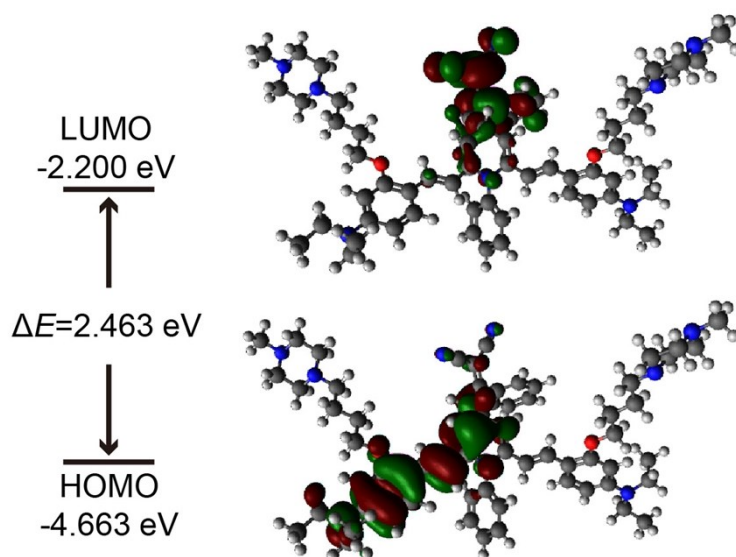


Fig. S3 HOMO and LUMO of TCM-PI by DFT calculations. The calculations were carried out using the Gaussian 09 program with the B3LYP functional and UB3LYP and the standard 6-31G* basis set. The lowest occupied molecular orbital (LUMO) was mainly localized at cyano unit (acceptor part), while the highest occupied molecular orbital (HOMO) concentrated on benzene ring with diethylamino group (donor part).

5. Measurement of solution's viscosity

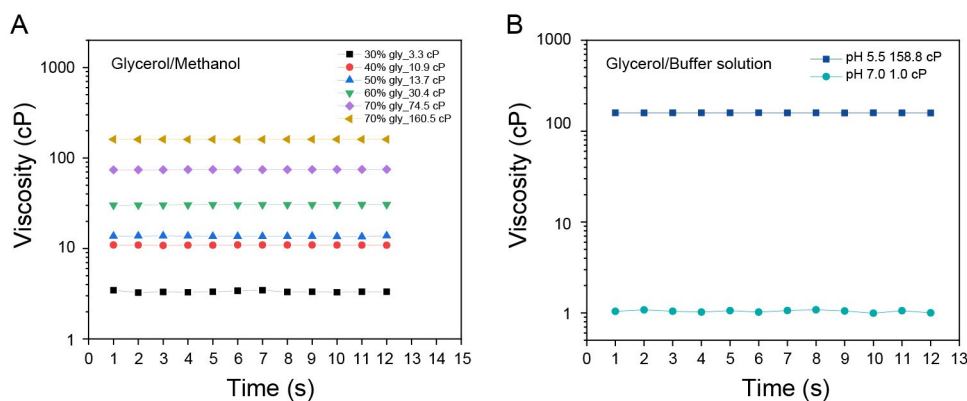


Fig. S4 (A) Measuring viscosity of glycerol/methanol mixtures with different volume fractions of glycerol. Test temperature: 25 °C. (B) Measuring viscosity of glycerol/Britton-Robinson buffer solution mixtures with different pH. Test temperature: 25 °C.

6. Photophysical property of TCM-PI in mixtures with different viscosity

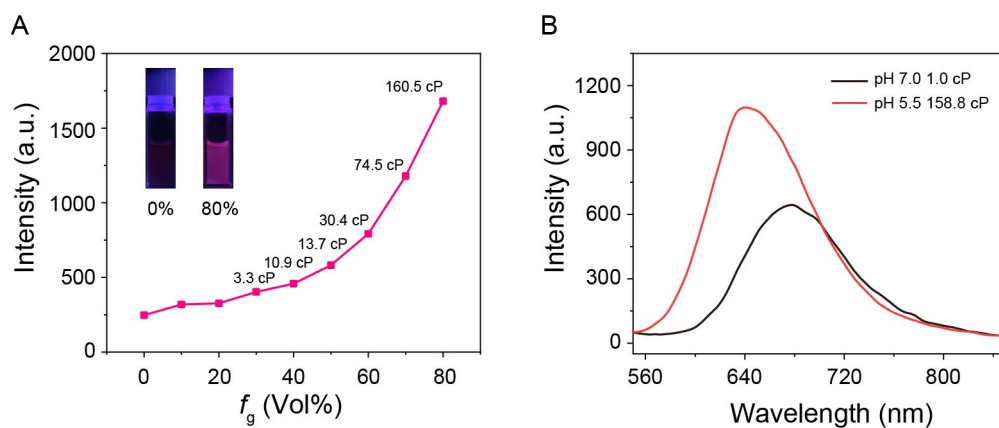


Fig. S5 (A) Plots of fluorescence intensity at emission peak versus volume fraction of glycerol (glycerol/methanol mixtures). Insert: photographs of TCM-PI in different glycerol fractions under illumination of UV lamp (365 nm). (B) Fluorescence emission spectrum of TCM-PI in pH 7.0 Britton-Robinson buffer solution with viscosity of 1.0 cP and pH 5.5 glycerol/Britton-Robinson buffer solution mixtures with viscosity of 159.0 cP. Concentration of TCM-PI on above experiment is 10 μ M.

7. Zeta potential of LysoTracker Red in water

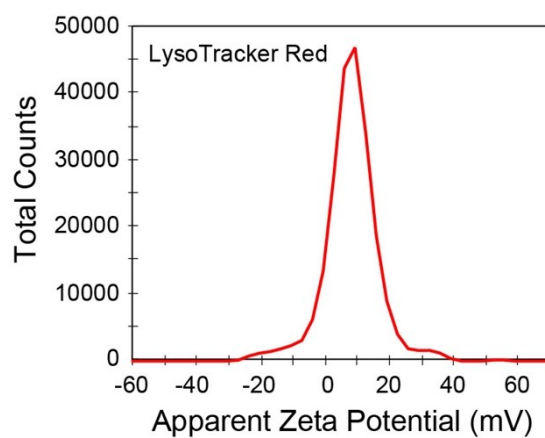


Fig. S6 Zeta potential of LysoTracker Red in water.

8. Size stability in pH 5.0 buffer solution and DMEM medium

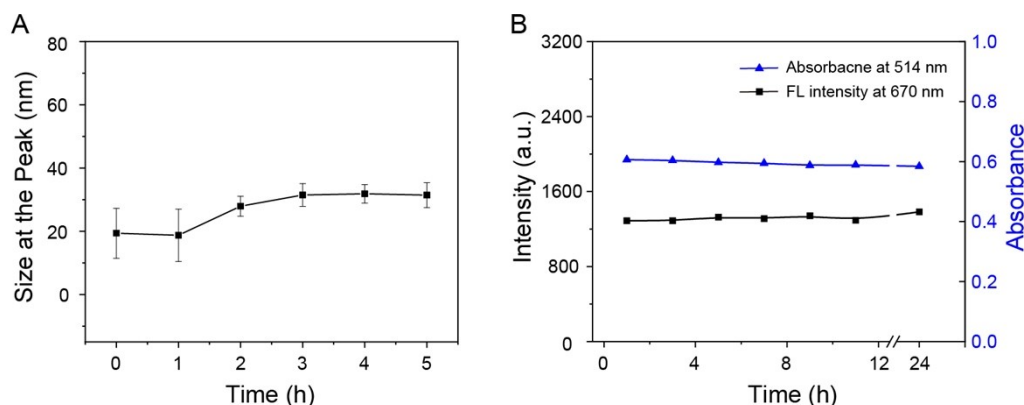


Fig. S7 (A) Size stability of TCM-PI nanoaggregates in 99% (Vol %) Britton-Robinson buffer solution with pH 5.0 at 37 °C for 5 h. Concentration: 10 μ M. (B) Plots of fluorescence intensity at 670 nm and absorbance at 514 nm of TCM-PI nanoaggregates in DMEM medium (supplemented with 10% fetal bovine serum and 1% penicillin-streptomycin solution) versus time at 37 °C.

9. Dynamic staining process of HeLa cells

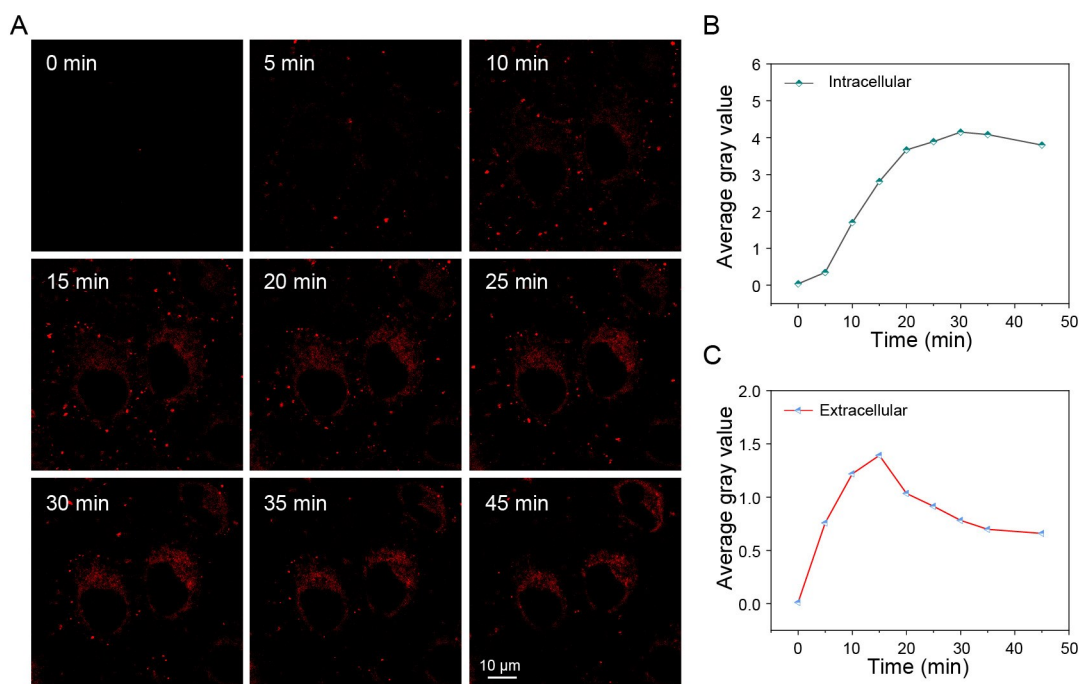


Fig. S8 (A) Dynamic staining process of HeLa cells incubated with TCM-PI (3 μ M) for 45 min. λ_{ex} =514 nm, λ_{em} =670-730 nm. (B) Intracellular average gray value versus time. (C) Extracellular average gray value versus time. Statistical data were obtained by photoshop.

10. Co-localization between TCM-PI nanoaggregates and LysoTracker Red

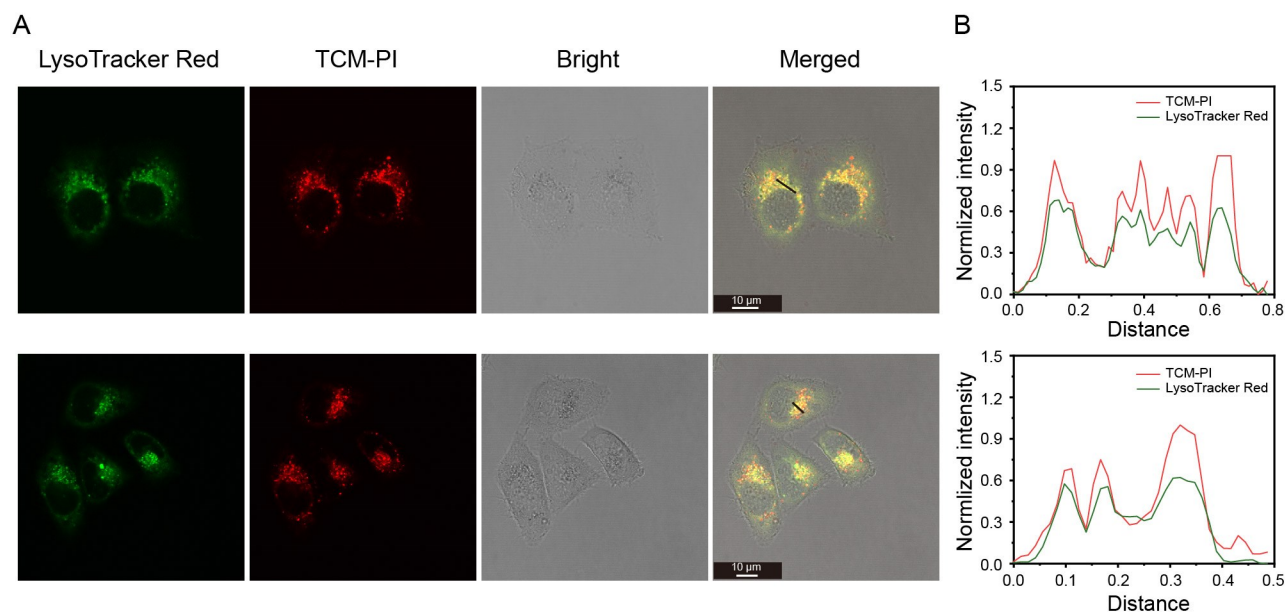


Fig. S9 (A) Confocal images of HeLa cells incubated with TCM-PI (3 μ M) for 30 minutes followed by co-staining with LysoTracker Red DND-99 (100 nM) for 30 min. Green Channel is from LysoTracker Red DND-99 (λ_{ex} =561 nm, λ_{em} =570-610 nm). Red Channel is from TCM-PI (λ_{ex} =514 nm, λ_{em} =670-730 nm). All confocal images share scale bar of 10 μ m. (B) Intensity profiles of the linear regions of interest (ROI) in the merged images.

11. 3D imaging of lysosomes with TCM-PI nanoaggregates

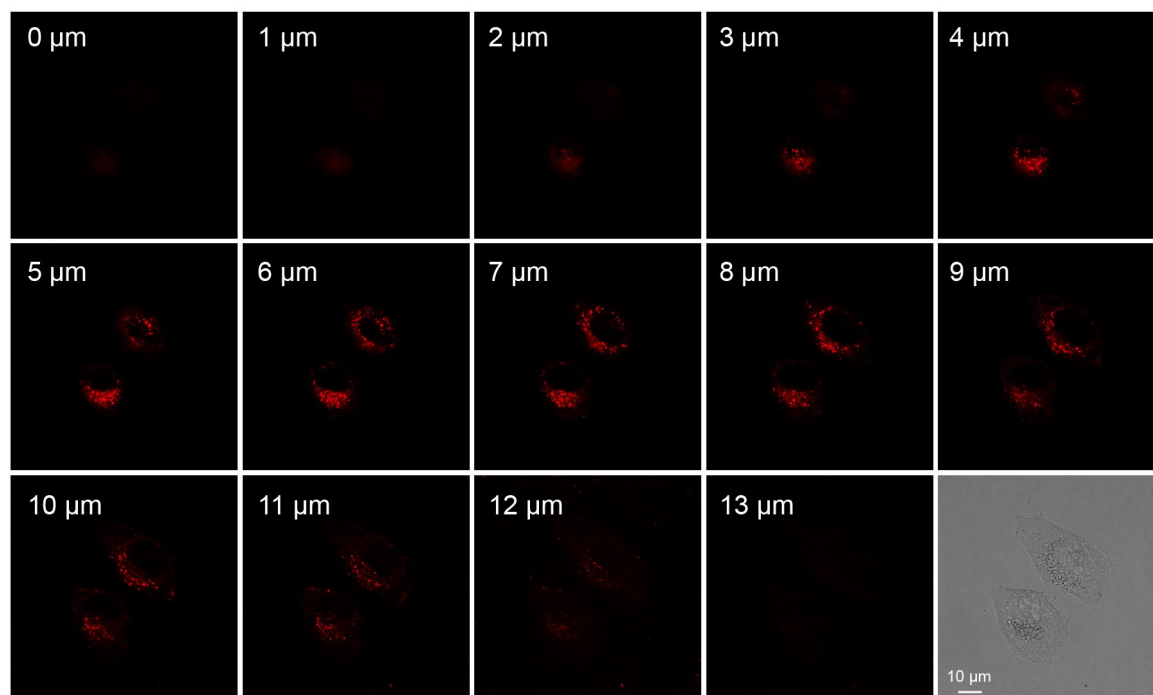


Fig. S10 3D slices of HeLa cells incubated with TCM-PI (3 μ M) for 30 minutes. Images are taken by laser

scanning confocal microscopy (Leica TCS SP8). All confocal images share scale bar of 10 μm . λ_{ex} =514 nm, λ_{em} =670-730 nm.

12. Biocompatibility of TCM-PI nanoaggregates

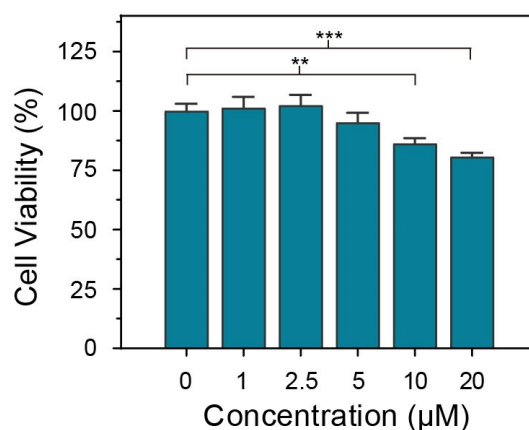


Fig. S11 Cell viability of HeLa cells versus the concentration of TCM-PI. Incubating time: 24 hours. Data are shown as mean \pm s.d., with $n = 3$. Statistical significance (p values, * represents $p < 0.05$, ** represents $p < 0.01$ and *** represents $p < 0.001$) was calculated with the Student's T-test.

13. Characterization of intermediate compounds and TCM-PI

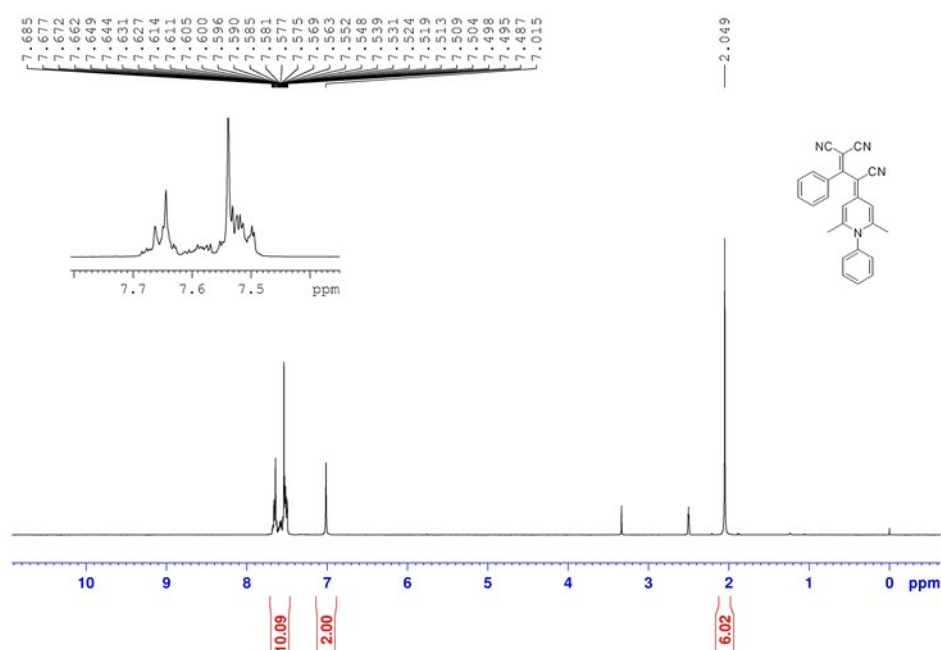


Fig. S12 ^1H NMR spectrum of TCM in $\text{DMSO-}d_6$.

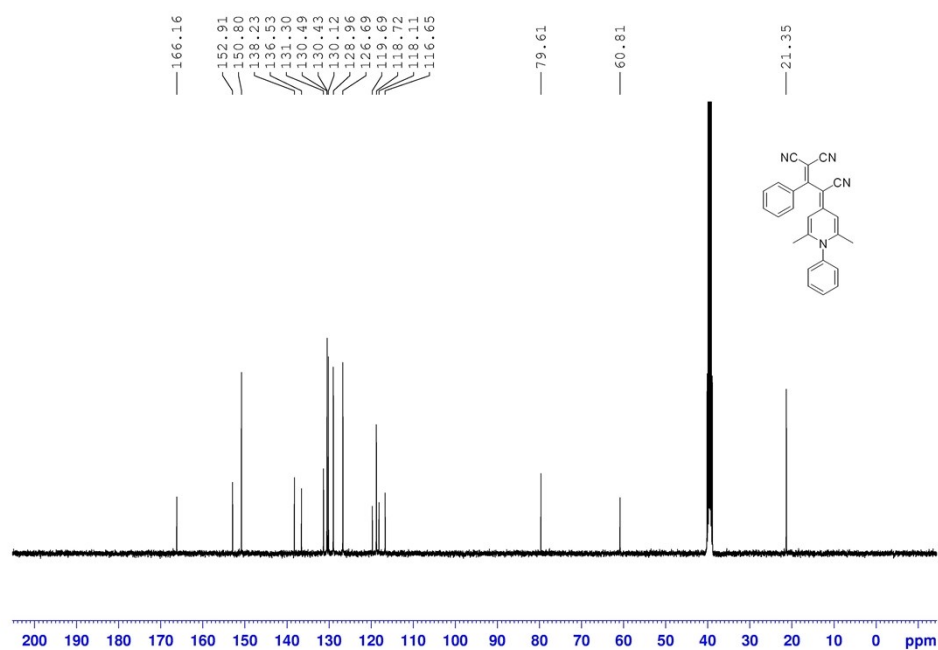


Fig. S13 ¹³C NMR spectrum of TCM in DMSO-*d*₆.

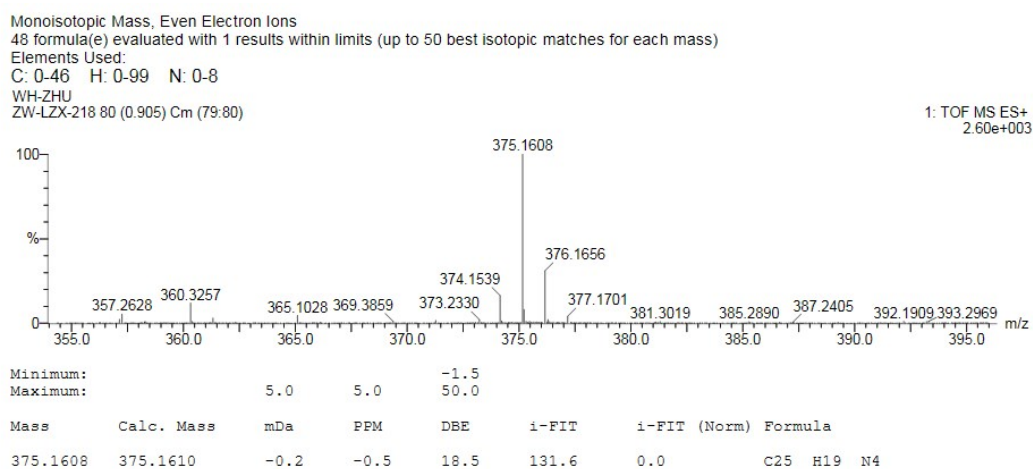


Fig. S14 HRMS spectrum of TCM.

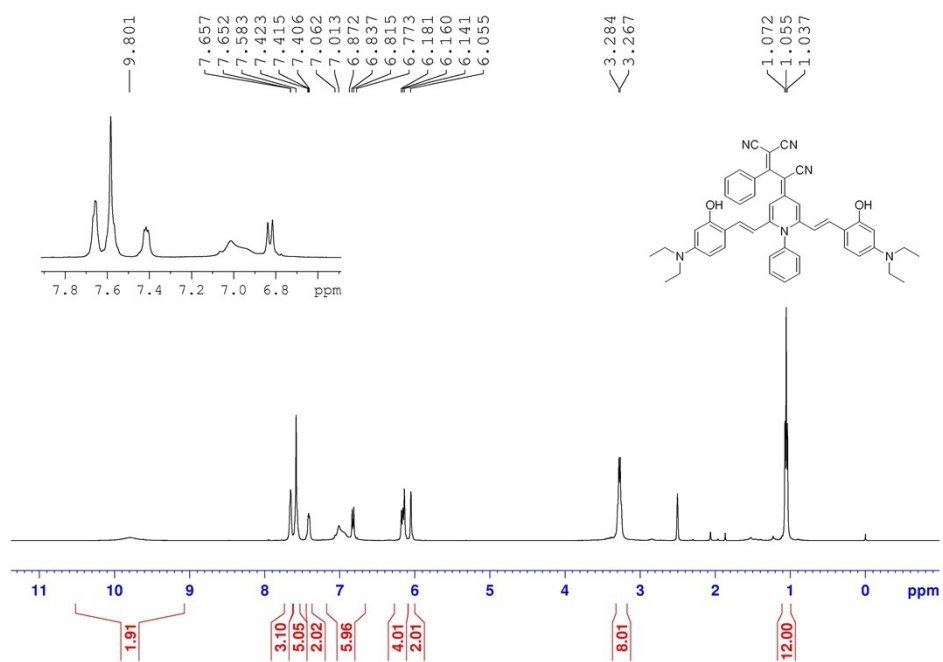


Fig. S15 ¹H NMR spectrum of TCM-NOH in DMSO-*d*₆.

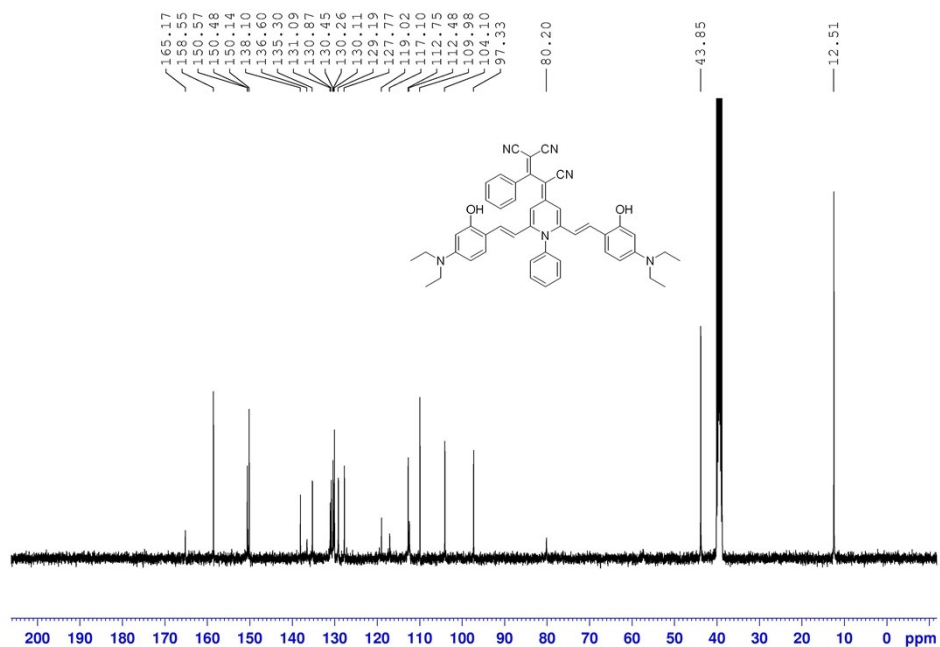
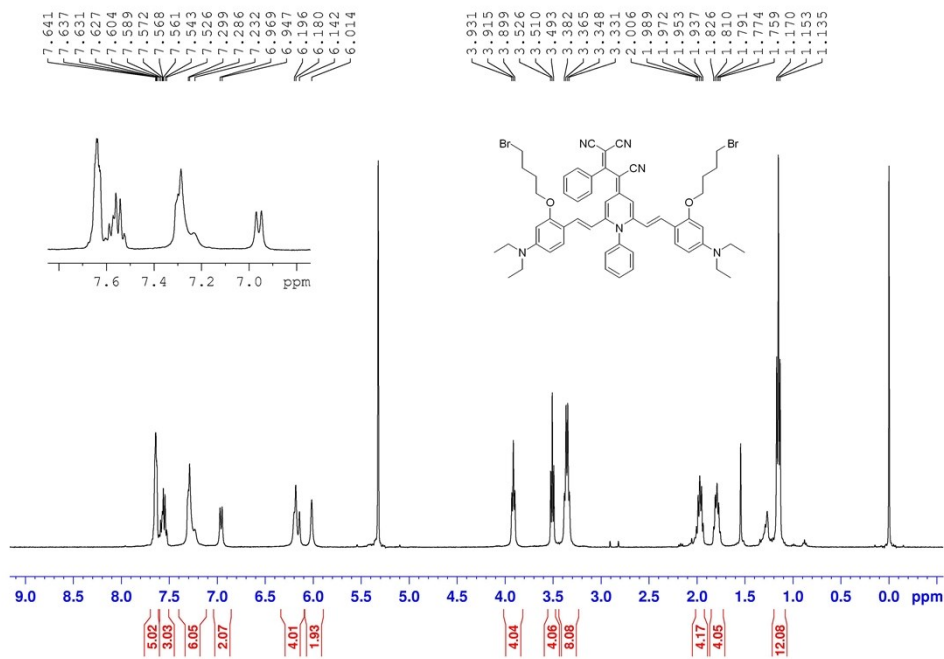
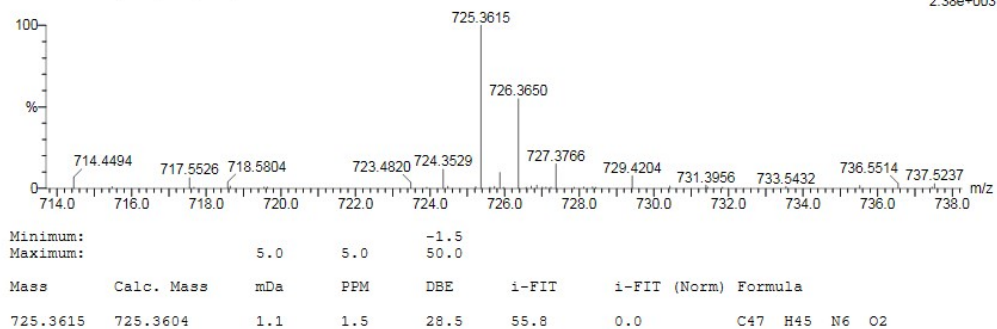


Fig. S16 ¹³C NMR spectrum of TCM-OH in DMSO-*d*₆.

1: TOF MS ES+
2.38e+003



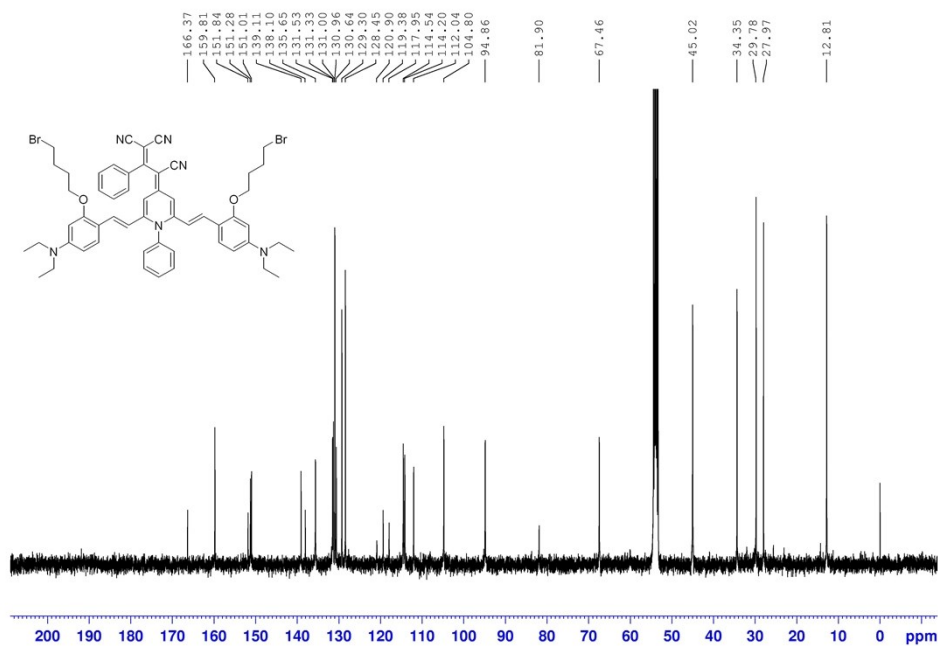


Fig. S19 ^{13}C NMR spectrum of TCM-NBr in $\text{CD}_2\text{Cl}_2-d_2$.

Monoisotopic Mass, Even Electron Ions

52 formula(e) evaluated with 1 results within limits (up to 50 best isotopic matches for each mass)

Elements Used:

C: 55-55 H: 0-66 N: 0-6 O: 0-2 Br: 0-2

WH-ZHU

ZW-LZX-308 66 (0.748) Cm (66.68)

1: TOF MS ES+
1.07e+003

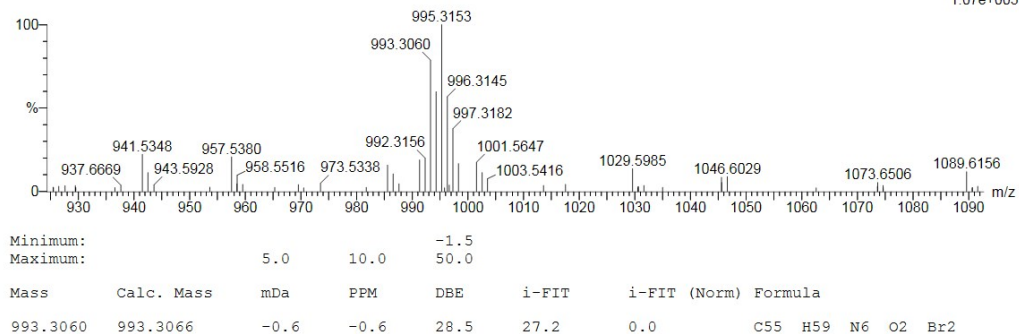


Fig. S20 HRMS spectrum of TCM-NBr.

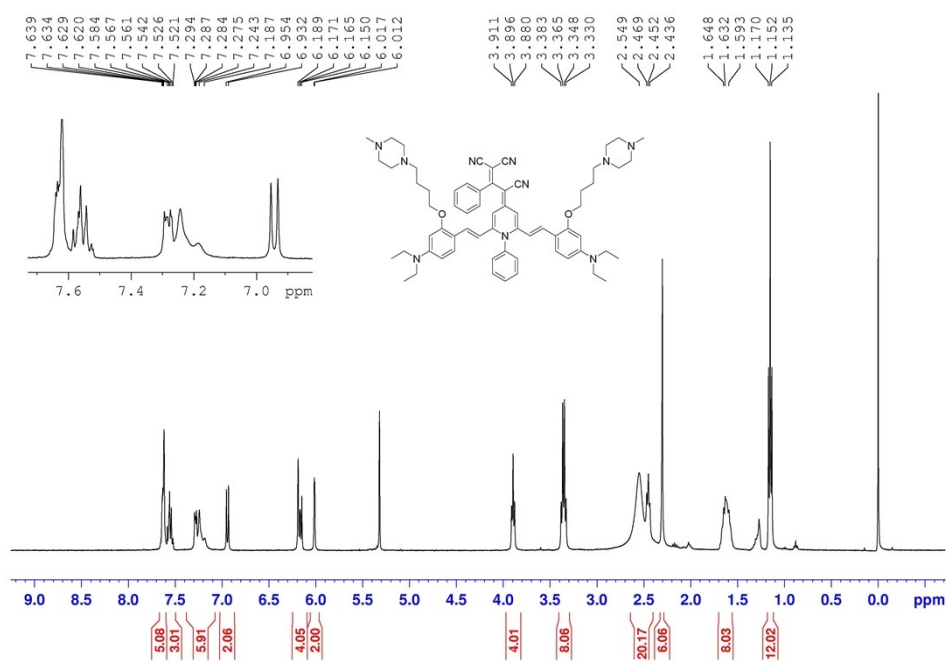


Fig. S21 ^1H NMR spectrum of TCM-PI in $\text{CD}_2\text{Cl}_2-d_2$.

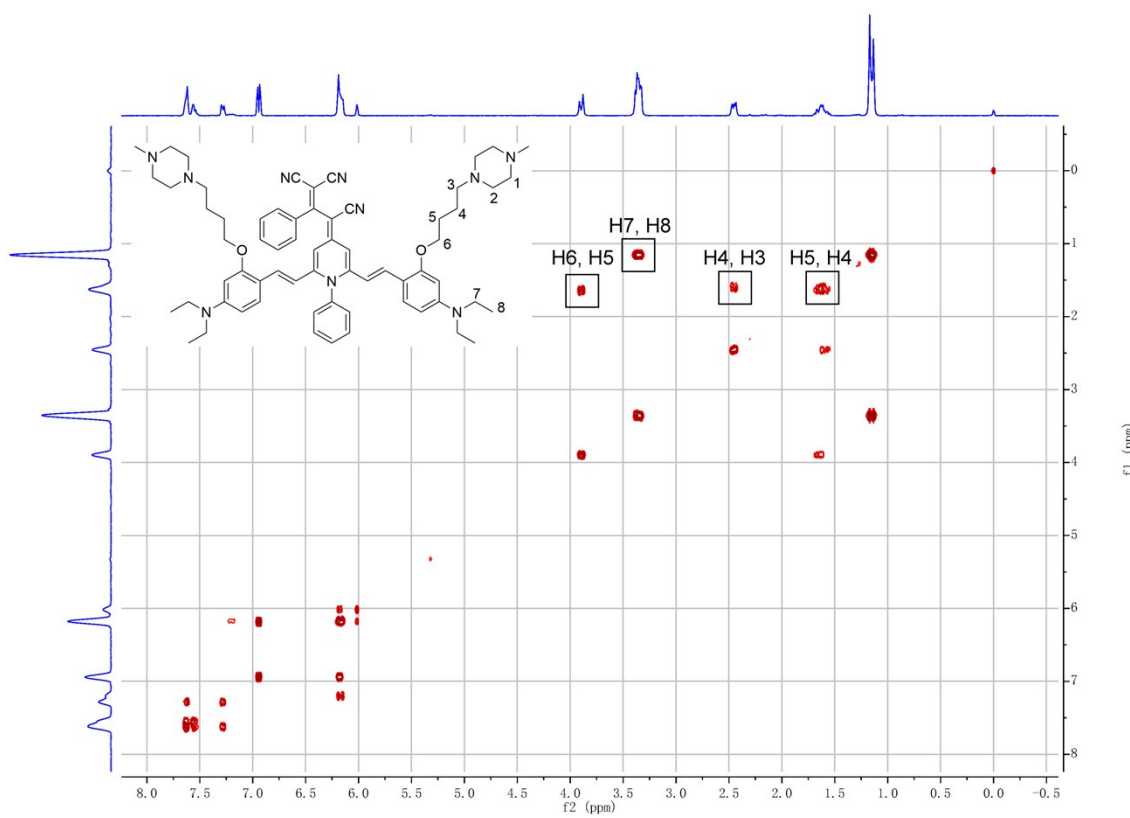


Fig. S22 Two-dimensional ^1H - ^1H COSY NMR spectrum of TCM-PI in $\text{CD}_2\text{Cl}_2-d_2$.

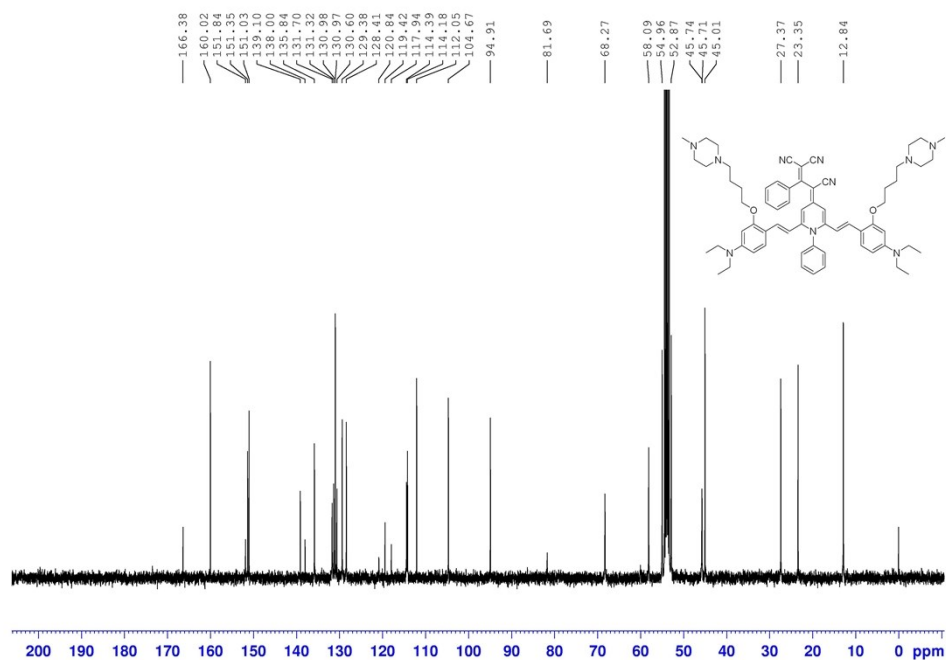


Fig. S23 ^{13}C NMR spectrum of TCM-PI in $\text{CD}_2\text{Cl}_2-d_2$.

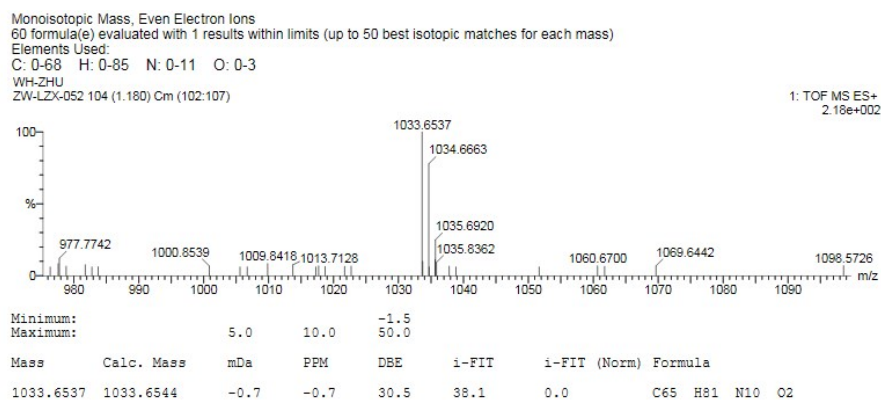


Fig. S24 HRMS spectrum of TCM-PI.

References

1. X. Wang, Z. Guo, S. Zhu, Y. Liu, P. Shi, H. Tian and W. H. Zhu, *J. Mater. Chem. B*, 2016, **4**, 4683-4689.